CICE 2023 Rio de Janeiro – Brazil 11TH INTERNATIONAL CONFERENCE ON FRP COMPOSITES IN CIVIL ENGINEERING

FATIGUE BEHAVIOR OF CFRP-CONCRETE JOINTS UNDER VARYING LOAD FREQUENCY

Tommaso D'Antino, Politecnico di Milano, Italy, tommaso.dantino@polimi.it
Massimiliano Bocciarelli, Politecnico di Milano, Italy, massimiliano.bocciarelli@polimi.it
Cristian Carloni, Case Western Reserve University, USA, christian.carloni@case.edu
Angelo Savio Calabrese, Politecnico di Milano, Italy, angelosavio.calabrese@polimi.it
Pierluigi Colombi, Politecnico di Milano, Italy, pierluigi.colombi@polimi.it
Tommaso Papa, Politecnico di Milano, Italy, tommaso.papa@polimi.it

ABSTRACT
Reinforced concrete structures are frequently subjected to fatigue loadings. At the interface between FRP and concrete, cyclic loading may induce the formation and coalescence of micro-cracks that result in the interface debonding. The stress transfer mechanism of the FRP-concrete bonded interface is critical to the performance of strengthened elements. This paper reports the preliminary results of an experimental investigation into the static and fatigue behavior of the interfacial bond between carbon fiber-reinforced polymer (CFRP) composite and a concrete substrate. Fatigue and post-fatigue loading curves were obtained to investigate the effect of the load frequency on the specimen response.

KEYWORDS
FRP laminates; direct-shear test; fatigue; frequency; bond behavior

INTRODUCTION
Crack propagation, induced by cyclic loading, is still an open issue relevant to many engineering applications, which requires further research work to investigate both its physical underlying mechanisms and the proper numerical approaches for its simulation (Nguyen et al., 2001; Roe & Siegmund, 2003). Fatigue crack propagation may occur in bulk material as well as in bonded joints, where high stress concentrations are present at the interface between two materials, inducing the formation of micro-cracks followed by crack coalescence resulting then in full detachment. This usually occurs for stress levels smaller than those causing debonding in quasi-static monotonic loading conditions.

The problem of fatigue induced crack propagation at the interface between two different materials is particularly relevant for externally bonded (EB) fiber-reinforced polymer (FRP) composites (Bocciarelli et al., 2013; Bocciarelli & Pisani, 2017). Carbon FRP (CFRP) have been recognized as an effective technique for the fatigue strengthening of both metallic and reinforced concrete structures (Bocciarelli et al., 2009; Hosseini et al., 2017), due to their corrosion resistance, light weight, and high strength and stiffness (Bocciarelli et al., 2014; Ghafoori & Motavalli, 2015). However, cyclic loading may induce CFRP-substrate interface debonding and drastically reduce the reinforcement effectiveness against fatigue crack propagation (Bocciarelli et al., 2018).

The resistance against fatigue is usually defined as the number of cycles of a certain amplitude and mean value that a structural element can withstand before failure. Different methods are currently used to estimate the fatigue resistance. These include: i) pure statistical approaches based on the analysis of experimental data (e.g., S-N curves) related to a specific structural detail or component (see, e.g. (Chalot et al., 2019; Paris & Erdogan, 1963; Zhu et al., 2016)); ii) fracture mechanics methods, where the rate of crack growth is defined as a function of some fracture mechanics parameters (such as the stress intensity factor or the strain energy release rate (Colombi & Fava, 2016; Kinloch & Osiyemi, 1993)), and iii) refined numerical approaches (see, e.g., (Martinelli & Caggiano, 2014)).

While extensive research was performed to study the behavior of FRP-concrete and FRP-steel joints under quasi-static monotonic loading, see e.g. (Barbieri et al., 2016; Bocciarelli et al., 2007), limited work was done to investigate the effect of cyclic loading. In (Ko & Sato, 2007; Mazzotti & Savoia, 2009), single- and double-lap direct shear tests were performed on FRP-concrete joints subjected to cyclic loadings. In (Carloni et al., 2012; Carloni & Subramaniam, 2013; Zhou et al., 2017), quasi-static single-lap direct shear tests were performed on FRP-concrete joints considering high-amplitude/low-cycle fatigue loading and measuring the strain distribution along the CFRP reinforcement with digital image correlation. Despite Ferrier et al. (Ferrier et al., 2005) observed that conventional civil engineering structures are typically loaded within a frequency range between 1 Hz and 5 Hz, the role of the cyclic loading frequency has not been fully investigated. The effect of bonded length, bonded width, and cyclic load value was investigated on CFRP-concrete joints subjected to cyclic loading, at a loading frequency equal to 1 Hz, in (Bizindavyi et al., 2003). The fatigue and post-fatigue behavior of small-scale beams strengthened with CFRP for various number of cycles and loading conditions was studied in (Gheorghiu et al., 2004, 2006, 2007). Although specimens were tested at 2 Hz and 3 Hz, the effect of frequency was not directly analyzed. Bond tests under 5 Hz cyclic loading were also performed in (Yun et al., 2008). Double-lap direct shear tests were employed to investigate the effect of fatigue loading on the crack growth rate along the FRP-concrete interface, observing a clear influence of the load frequency on the bond degradation (Diab et al., 2009). In addition to the limited experimental results, available data are not easily comparable due to the different set-up and frequencies adopted.
In this paper, the preliminary results of an ongoing experimental campaign aimed at investigating the static and fatigue behavior of CFRP-concrete joints are presented. Seven single-lap direct shear specimens were tested under quasi-static monotonic and cyclic loading with different cyclic load values and frequencies. The effect of cyclic load frequency on the interface slip, area of cycles, and post-fatigue bond capacity was investigated for different cyclic load values.

MATERIALS AND METHODS

Seven FRP-concrete joints were tested using a single-lap direct shear test configuration. Three specimens were tested with a quasi-static monotonic load, whereas four specimens were tested with a cyclic load for a certain number of cycles, after which they were tested with a quasi-static monotonic load until failure. The FRP-concrete joints were comprised of concrete blocks and carbon FRP (CFRP) strips. The seven concrete blocks had length equal to 300 mm and 100×100 mm cross-section and were cast from the same concrete batch. The concrete compressive strength was measured by compressive tests of three 150 mm-side cubes that provided an average concrete strength R_{cm}=29.1 MPa (CoV=3.93%), which corresponds to an average cylindrical strength $f_{cm}=0.83\times R_{cm}$=24.1 MPa. The carbon FRP strips were comprised of a dry unidirectional fiber sheet with an area weight of 300 g/m^2 (equivalent thickness t_f=0.166 mm), laminated using the wet lay-up method. The mean tensile strength f_f and elastic modulus E_f of the composite were f_f=3570 MPa and E_f=225 GPa, as declared by the manufacturer (Sika Italia SpA, 2019). The strips were bonded onto the bottom face of the concrete block, i.e., the face opposite to the casting face, using a bi-component epoxy resin specifically designed for application onto concrete substrates (Sika Italia SpA, 2019).

The FRP-concrete joints were realized following the indications of ASTM D8337/D8337M-21 (ASTM International, 2021). The concrete surface was first roughened using a pneumatic jack hammer and then accurately cleaned with air. Four specimens were realized at the same time, using the other four blocks to accurately align the CFRP strip during the wet lay-up procedure, as suggested by ASTM D8337/D8337M-21 (ASTM International, 2021). The strip bonded length and width were ℓ =200 mm and b_f=50 mm, respectively (Figure 1). The bonded area was placed 70 mm far from the concrete block edge to avoid wedge failure. The bonded length was selected to be higher than the joint effective bond length, i.e., the minimum length needed to fully establish the interface stress transfer mechanism, according to the formula provided by Chen and Teng (Chen & Teng, 2001). The portion of composite not bonded to the concrete block had a length of 370 mm. Two glass FRP tabs were epoxy bonded to the strip end to facilitate gripping by the testing machine. The concrete block was fixed to the laboratory strong floor using steel profiles, while the CFRP strip was pulled using a servo-hydraulic jack equipped with a 100 kN load cell. The CFRP-concrete relative displacement at

the loaded end was measured using two LVDTs with stroke 10 mm attached to the concrete block at the loaded end. The LVDTs reacted off an omega-shaped steel plate attached to the CFRP strip (Figure 1). The average of the displacements measured by the two LVDTs is named global slip *g*. Quasi-static monotonic phases of the tests were conducted in stroke- or global slip-control. In the former case, the stroke was controlled at a constant rate equal to 0.005 mm/s, while in the latter the global slip was controlled at a constant rate equal to 0.001 mm/s (ASTM International, 2021). The test cyclic phase was conducted in force-control at a load frequency equal to 1 or 5 Hz.

Specimens tested with a quasi-static load were named following the notation DS_L_W_n, where DS=direct shear test, L=bonded length (in mm), W=bonded width (in mm), and n=specimen number. Specimens tested with a cyclic load were named following the notation DSF_f_P_v-P_p_n, where DSF=fatigue direct shear test, f=load frequency, P_v and P_p are the minimum (valley) and maximum (peak) loads applied during the cyclic test expressed as percentages of the average bond capacity $P_{pl,avg}$ obtained by corresponding quasi-static tests, and n=specimen number. The specimens tested are reported in Table 1.

Table 1: Specimens tested

Specimens	*f* [Hz]	P^* [kN]	P_{pl} [kN]	σ^*[MPa]	P_v [kN]	P_p [kN]	P_m [kN]	P_{amp} [kN]	N_F [-]
DS_200_50_1		11.30	9.45	1353					
DS_200_50_2		9.97	9.42	1194					
DS_200_50_3		10.04	9.68	1202					
Average		10.43	9.51	1250					
CoV [%]		5.86	1.22	5.86					
DSF_1_35-65_1	1	13.32	12.35	1595	3.33	6.18	4.76	1.43	111,110
DSF_5_35-65_1	5	13.96	13.12	1671	3.33	6.18	4.76	1.43	1,251,110
DSF_1_20-65_1	1	12.30	10.92	1473	1.90	6.18	4.04	2.14	111,110
DSF_5_20-65_1	5	14.39	12.78	1724	1.90	6.18	4.04	2.14	1,411,110
Average		13.49	12.29	1616					
CoV [%]		5.83	6.83	5.83					

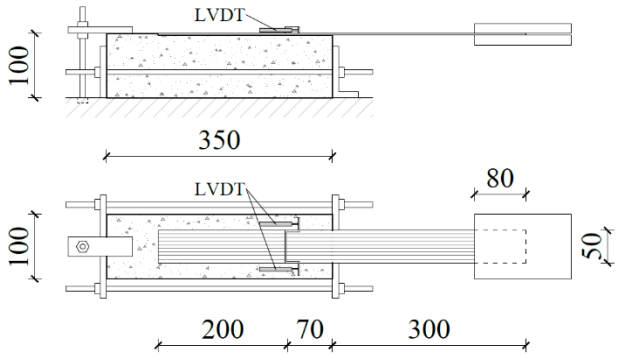

Figure 1: Single-lap direct sherar test set-up (dimensions in mm)

RESULTS AND DISCUSSION

Quasi-static tests

Three specimens were tested with a quasi-static monotonic load to determine the parameters needed for fatigue tests. The first two specimens, namely DS_200_50_1 and 2, were tested in stroke control, while specimen DS_200_50_3 was tested in global slip control. All specimens failed due to debonding within a thin layer of concrete. An image of failure of specimen DS_200_50_1 is shown in Figure 2a. The applied load *P* – global slip *g* responses obtained are shown in Figure 2b, where the applied stress $\sigma=P/(b_f t_f)$ is shown in the secondary vertical axes. All specimens provided a consistent

behavior, with an initial approximately linear ascending branch followed by a non-linear branch and a final branch where the applied load remained approximately constant. This behavior is typical of FRP-concrete joints with bonded length higher than the effective bond length (ASTM International, 2021). The portion of load response where the stress transfer was fully established and the applied load remained approximately constant was more pronounced in specimen DS_200_50_3 than in the other specimens. This difference was attributed to the different test control mode adopted. The global slip control allowed for accurately capturing the interface crack propagation, as can be noticed by several applied load drops in Figure 2b. The stroke control could not follow the interface crack propagation with the same accuracy and did not allow for accurately capturing the load plateau.
In specimen DS_200_50_3, the applied load associated with the onset of debonding could be identified as that followed by a load drop and then by the load plateau (Figure 2b). According to the definition of ASTM D8337/D8337M-21 (ASTM International, 2021), the bond capacity P_{pl} of specimen DS_200_50_3 was computed as the average load within the interval g_1-g_2, where g_1 is the global slip associated with the minimum force of the load drop following the onset of debonding and g_2 with the beginning of the last ascending branch preceding the specimen failure. Since specimens DS_200_50_1 and 2 were stroke-controlled and it was not possible to clearly identified g_1-g_2, the bond capacity was computed as the average load between the interval g_1-g_2 obtained for specimen DS_200_50_3. The average bond capacity of the three quasi-static tests was $P_{pl,avg}$=9.51 kN (see Table 1 and Figure 2b). The maximum load P^* and stress σ^*, as well as the corresponding coefficients of variation CoV, are reported in Table 1 for each specimen.

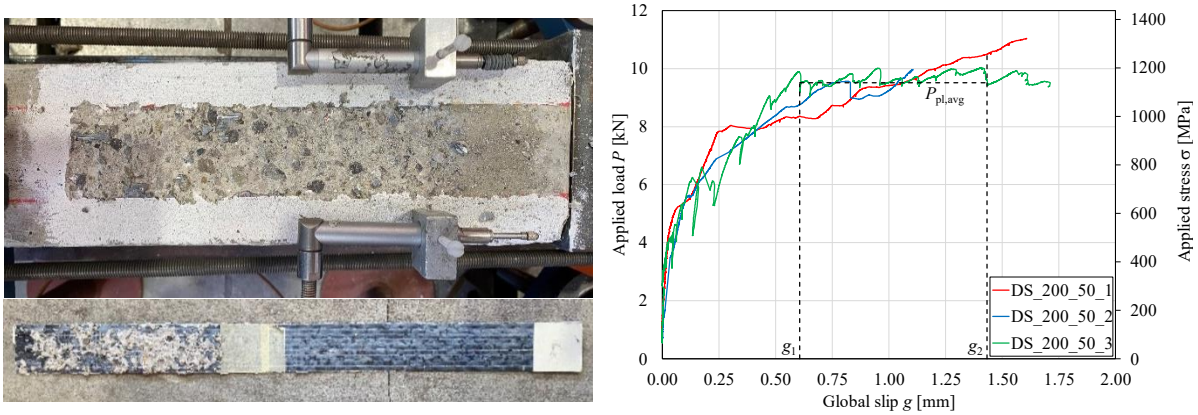

a) b)

Figure 2: a) Failure of specimen DS_200_50_1 and b) load responses of specimens tested with a quasi-static load

Fatigue tests

Four specimens were tested under a cyclic loading. Two load ranges were considered, namely $0.35P_{pl,avg}$ - $0.65P_{pl,avg}$ and $0.20P_{pl,avg}$ - $0.65P_{pl,avg}$. The fatigue valley (P_v) and peak (P_p) applied loads, mean fatigue load P_m, and fatigue load amplitude P_{amp} are reported in Table 1 for each specimen. For a given load range, one specimen was tested with a cycle frequency of 1 Hz, while the other with a cycle frequency of 5 Hz. In the first phase of fatigue tests, CFRP-concrete joints were subjected to a quasi-static monotonic stroke-controlled test until the peak fatigue load P_p was reached. Then, the stroke was decreases at a rate of 0.005 mm/s until the mean fatigue load was attained. At this point, the fatigue test was started using the load frequency selected. After a certain number of cycles N_F (see Table 1), the fatigue test was interrupted and the specimen tested under quasi-static global slip control until failure. Only for specimen DSF_5_35-65_1, the post fatigue test was performed in stroke control to assess the difference with respect to the other specimens. Due to the different frequencies considered, the fatigue phase of specimens tested at 1 Hz was interrupted at N_F=111,110, whereas more than 1 million cycles were applied to specimens tested at 5 Hz (see Table 1). During the fatigue phase, at fixed number of cycles, the cyclic test was interrupted and the specimen un-loaded and re-loaded in quasi-static global slip control to investigate the propagation of the debonding crack (if

any). Then, the fatigue test was re-started. The analysis of the debonding crack propagation is not provided in this paper.

Figure 3 shows the load response of specimen DSF_1_35_65_1, which is representative of load responses obtained. In Figure 3a, the first test phase until P_p and the following decreases to the mean fatigue load are shown. In addition, blocks of 10 fatigue cycles for N=10, 100, 1,000, 10,000, and 100,000 are provided in Figure 3a. These 10-cycle blocks showed that g increased and the area within each cycle varied with increasing N. Figure 3b shows the entire test, including the 10-cycle blocks showed in Figure 3a and the last 10 cycles before the beginning of the post-fatigue test. The post-fatigue load response observed had a behavior consistent with those observed in quasi-static tests. All specimens failed due to debonding within a thin layer of concrete, as observed in specimens DS_200_50_1-3 (see failure of specimen DSF_1_35_65_1 in Figure 4, which is representative of the failure mode observed).

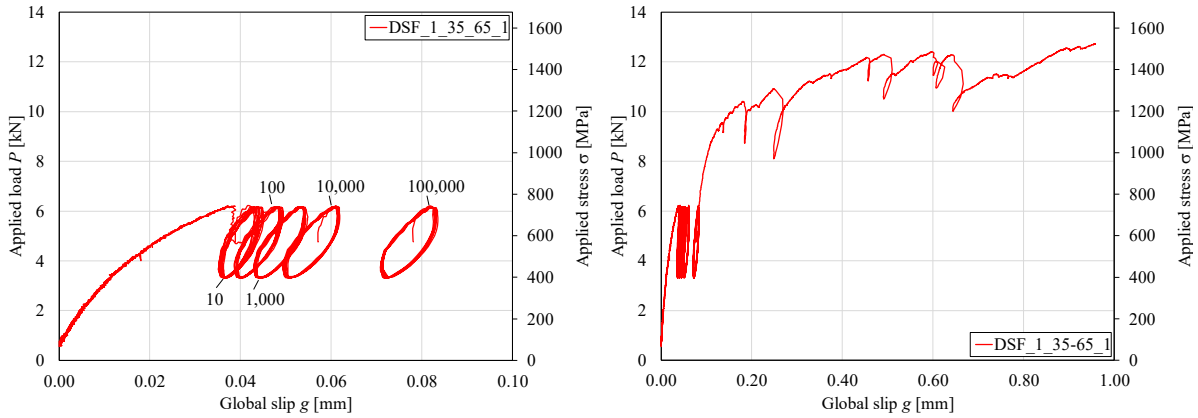

a) b)

Figure 3: Load response of specimen DSF_1_35-65_1: a) initial loading phase and representative 10-cycle blocks; and b) initial loading phase, representative 10-cycle blocks, and post-fatigue response

Figure 4: Failure of specimen DSF_1_35-65_1

The effect of the fatigue frequency on the specimen response was investigated analysing the variation of the global slip g and area within the fatigue cycle, with respect to the number of cycles N. In Figure 5a, the normalized global slip g/g_0, where g_0 is the global slip at the end of the first quasi-static phase, was plot with respect to the number of cycles N for all fatigue specimens. The ratio g/g_0 was computed for the same number of cycles considered for the 10-cycle blocks depicted in Figure 3a and for $N=N_F$. Considering specimens with the lowest fatigue amplitude, g/g_0 increased with a higher rate for the specimen with load frequency f=1 Hz than for that with f=5 Hz. However, g/g_0 was higher for specimen DSF_5_35-65_1 than for specimen DSF_1_35-65_1 when N=111,110. An opposite trend was observed in specimens with the highest fatigue amplitude. For N≤11,110, values of g/g_0 higher for f=5 Hz than for f=1 Hz were observed. Afterward, specimen DSF_1_20-65_1 showed a sudden increase of g/g_0, whereas the increase rate observed in specimen DSF_5_20-65_1 tended to decrease with increasing N. The results obtained did not allow for drawing clear conclusions on the effect of the fatigue frequency on the global slip. Further tests are needed to clarify this aspect.

The cycle area A was computed as the average area of a 10-cycle block. The normalized cycle area A/A_0, where A_0 is the average cycle area associated with the first 10 cycles of the fatigue phase, is plotted versus the number of cycles N in Figure 5b. A/A_0 was computed for the same number of cycles considered for g/g_0. In this case, a different behavior was observed depending on the cyclic load value. For specimens with the lowest amplitude, the highest frequency was associated with the lowest normalized cycle area for the same number of cycles. An opposite trend was observed on specimens with the highest amplitude, where larger normalized cycle area values were provided by specimen DSF_5_20-65_1 than for specimen DSF_1_20-65_1. This result suggests that the fatigue load level and frequency might affect the specimen behavior.

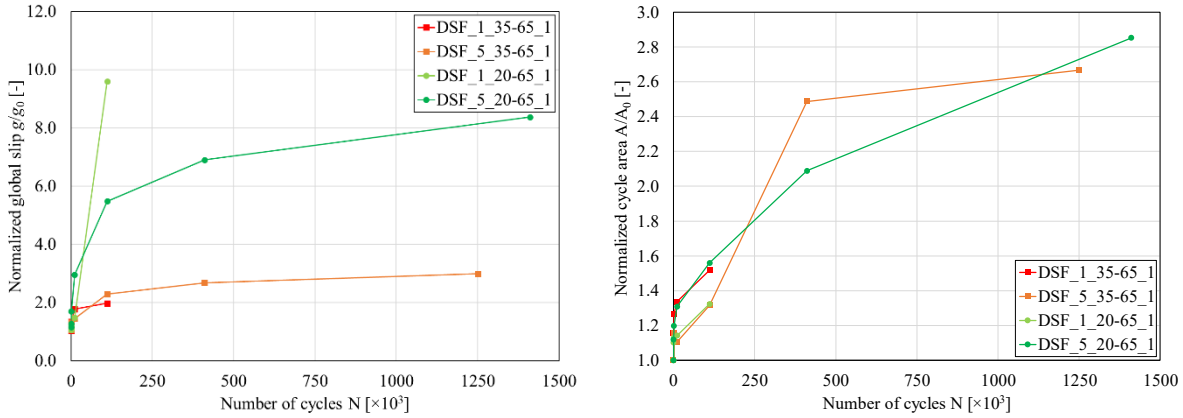

a) b)

Figure 5: a) Normalized global slip and b) normalized cycle area versus the number of cycles

The post-fatigue load responses of the specimens tested are shown in Figure 6, whereas the load plateau P_{pl} of each specimen, the average load plateau $P_{pl,avg}$, and the corresponding CoV are provided in Table 1. According to ASTM D8337/D8337M-21 (ASTM International, 2021), P_{pl} was obtained as the average load between g_1 and g_2, which for global slip-controlled tests were determined as the global slips associated with the minimum applied load after the onset of debonding and the minimum load preceding the last increasing branch, respectively. For specimen DSF_5_35-65_1 (stroke-controlled), g_1 was the global slip associated with the maximum applied load and g_2 the last value before failure (ASTM International, 2021).

Although the post fatigue load responses had a behavior consistent with that of load responses of quasi-static specimens (Figure 2), $P_{pl,avg}$ was 29.2% higher in the former than in the latter case. Since the CFRP-concrete joints were nominally equal (CFRP strips taken from the same roller and applied with the same epoxy resin to the bottom face of blocks belonging to the same concrete batch), this difference could be attributed to the result scatter. Further investigations will be performed to determine the effect of fatigue cycles on the specimen post fatigue response.

As previously observed for quasi-static tests, the stroke control provided a load response different from that obtained with the global-slip control. Namely, the propagation of the debonding crack could not be accurately followed in specimen DSF_5_35-65_1, while it was captured in the other specimens, as shown by numerous load drops in Figure 6. This confirms the importance of conducting the test in global-slip control to obtain detailed information on the debonding process.

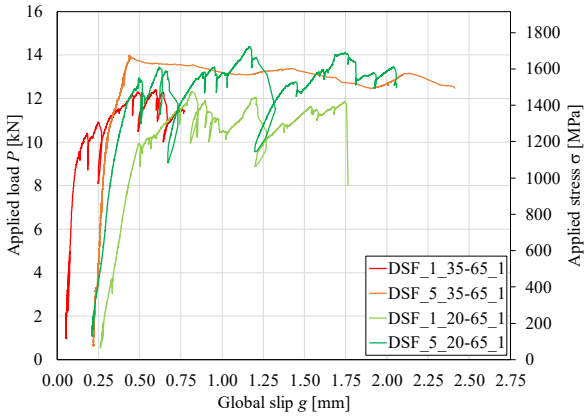

Figure 6: Comparison between post-fatigue load responses of specimens tested

CONCLUSIONS

In this paper, the quasi-static and fatigue behavior of CFRP strips applied onto a concrete substrate was studied considering single-lap direct shear tests of CFRP-concrete joints. Three specimens were tested with a quasi-static load. Four specimens were tested with a cyclic load for a certain number of cycles and then with a quasi-static load until failure. Cyclic loads with two different amplitudes and mean loads and two different frequencies were considered. The results obtained showed that the fatigue frequency affects the variation of the global slip with the number of cycles, although contradictory trends were observed depending on the fatigue load range considered. Similarly, the variation of the area within the fatigue cycle appeared to be affected by the fatigue frequency and load value. Finally, post fatigue responses showed a behavior consistent with that of quasi-static specimens, although with a higher bond capacity. This difference was attributed to the results scatter. Further tests are needed to clarify the effect of fatigue frequency on the global slip behavior and on the post fatigue response.

ACKNOWLEDGEMENTS

The experimental tests described in this paper were carried out at the Reparto Ancoraggi of the Laboratorio Prove Materiali, Politecnico di Milano, Italy.

CONFLICT OF INTEREST

The authors declare that they have no conflicts of interest associated with the work presented in this paper.

DATA AVAILABILITY

Data on which this paper is based is available from the authors upon reasonable request.

REFERENCES

ASTM International. (2021). Standard Test Method for Evaluation of Bond Properties of FRP Composite Applied to Concrete Substrate using Single-Lap Shear Test. ASTM D8337/D8337M-21. ASTM International. https://www.astm.org/d8337_d8337m-21.html

Barbieri, G., Biolzi, L., Bocciarelli, M., & Cattaneo, S. (2016). Size and shape effect in the pull-out of FRP reinforcement from concrete. Composite Structures, 143, 395–417. https://doi.org/10.1016/j.compstruct.2016.01.097

Bizindavyi, L., Neale, K. W., & Erki, M. A. (2003). Experimental Investigation of Bonded Fiber Reinforced Polymer-Concrete Joints under Cyclic Loading. Journal of Composites for Construction, 7(2), 127–134. https://doi.org/10.1061/(ASCE)1090-0268(2003)7:2(127)

Bocciarelli, M., Colombi, P., D'Antino, T., & Fava, G. (2018). Intermediate crack induced debonding in steel beams reinforced with CFRP plates under fatigue loading. Engineering Structures, 171, 883–893. https://doi.org/10.1016/j.engstruct.2018.04.002

Bocciarelli, M., Colombi, P., Fava, G., & Poggi, C. (2007). Interaction of interface delamination and plasticity in tensile steel members reinforced by CFRP plates. International Journal of Fracture, 146(1), 79–92. https://doi.org/10.1007/s10704-007-9144-8
Bocciarelli, M., Colombi, P., Fava, G., & Poggi, C. (2009). Fatigue performance of tensile steel members strengthened with CFRP plates. Composite Structures, 87(4), 334–343. https://doi.org/10.1016/j.compstruct.2008.02.004
Bocciarelli, M., Feo, C. di, Nisticò, N., Pisani, M. A., & Poggi, C. (2013). Failure of RC beams strengthened in bending with unconventionally arranged CFRP laminates. Composites Part B: Engineering, 54, 246–254. https://doi.org/10.1016/j.compositesb.2013.05.028
Bocciarelli, M., Gambarelli, S., Nisticò, N., Pisani, M. A., & Poggi, C. (2014). Shear failure of RC elements strengthened with steel profiles and CFRP wraps. Composites Part B: Engineering, 67, 9–21. https://doi.org/10.1016/j.compositesb.2014.06.009
Bocciarelli, M., & Pisani, M. A. (2017). Survey on the interface behaviour in reinforced concrete beams strengthened with externally bonded FRP reinforcement. Composites Part B: Engineering, 118, 169–176. https://doi.org/10.1016/j.compositesb.2017.02.047
Carloni, C., & Subramaniam, K. V. (2013). Investigation of sub-critical fatigue crack growth in FRP/concrete cohesive interface using digital image analysis. Composites Part B: Engineering, 51, 35–43. https://doi.org/10.1016/j.compositesb.2013.02.015
Carloni, C., Subramaniam, K. V., Savoia, M., & Mazzotti, C. (2012). Experimental determination of FRP–concrete cohesive interface properties under fatigue loading. Composite Structures, 94(4), 1288–1296. https://doi.org/10.1016/j.compstruct.2011.10.026
Chalot, A., Michel, L., & Ferrier, E. (2019). Experimental study of external bonded CFRP-concrete interface under low cycle fatigue loading. Composites Part B: Engineering, 177, 107255. https://doi.org/10.1016/j.compositesb.2019.107255
Chen, J. F., & Teng, J. G. (2001). Anchorage Strength Models for FRP and Steel Plates Bonded to Concrete. Journal of Structural Engineering, 127(7), 784–791. https://doi.org/10.1061/(ASCE)0733-9445(2001)127:7(784)
Colombi, P., & Fava, G. (2016). Fatigue crack growth in steel beams strengthened by CFRP strips. Theoretical and Applied Fracture Mechanics, 85, 173–182. https://doi.org/10.1016/j.tafmec.2016.01.007
Diab, H. M., Wu, Z., & Iwashita, K. (2009). Theoretical Solution for Fatigue Debonding Growth and Fatigue Life Prediction of FRP-Concrete Interfaces. Advances in Structural Engineering, 12(6), 781–792. https://doi.org/10.1260/136943309790327707
Ferrier, E., Bigaud, D., Hamelin, P., Bizindavyi, L., & Neale, K. W. (2005). Fatigue of CFRPs externally bonded to concrete. Materials and Structures, 38(1), 39–46. https://doi.org/10.1007/BF02480573
Ghafoori, E., & Motavalli, M. (2015). Innovative CFRP-Prestressing System for Strengthening Metallic Structures. Journal of Composites for Construction, 19(6), 04015006. https://doi.org/10.1061/(ASCE)CC.1943-5614.0000559
Gheorghiu, C., Labossière, P., & Proulx, J. (2006). Fatigue and monotonic strength of RC beams strengthened with CFRPs. Composites Part A: Applied Science and Manufacturing, 37(8), 1111–1118. https://doi.org/10.1016/j.compositesa.2005.05.035
Gheorghiu, C., Labossière, P., & Proulx, J. (2007). Response of CFRP-strengthened beams under fatigue with different load amplitudes. Construction and Building Materials, 21(4), 756–763. https://doi.org/10.1016/j.conbuildmat.2006.06.019
Gheorghiu, C., Labossière, P., & Raıχche, A. (2004). Environmental Fatigue and Static Behavior of RC Beams Strengthened with Carbon-Fiber-Reinforced Polymer. Journal of Composites for Construction, 8(3), 211–218. https://doi.org/10.1061/(ASCE)1090-0268(2004)8:3(211)
Hosseini, A., Ghafoori, E., Motavalli, M., Nussbaumer, A., & Zhao, X.-L. (2017). Mode I fatigue crack arrest in tensile steel members using prestressed CFRP plates. Composite Structures, 178, 119–134. https://doi.org/10.1016/j.compstruct.2017.06.056
Kinloch, A. J., & Osiyemi, S. O. (1993). Predicting the Fatigue Life of Adhesively-Bonded Joints. The Journal of Adhesion, 43(1–2), 79–90. https://doi.org/10.1080/00218469308026589

Ko, H., & Sato, Y. (2007). Bond Stress–Slip Relationship between FRP Sheet and Concrete under Cyclic Load. Journal of Composites for Construction, 11(4), 419–426. https://doi.org/10.1061/(ASCE)1090-0268(2007)11:4(419)

Martinelli, E., & Caggiano, A. (2014). A Unified Theoretical Model for the Monotonic and Cyclic Response of FRP Strips Glued to Concrete. Polymers, 6(2), 370–381. https://doi.org/10.3390/polym6020370

Mazzotti, C., & Savoia, M. (2009). FRP-Concrete Bond Behaviour under Cyclic Debonding Force. Advances in Structural Engineering, 12(6), 771–780. https://doi.org/10.1260/136943309790327761

Nguyen, O., Repetto, E. A., Ortiz, M., & Radovitzky, R. A. (2001). A cohesive model of fatigue crack growth. International Journal of Fracture, 110(4), 351–369. https://doi.org/10.1023/A:1010839522926

Paris, P., & Erdogan, F. (1963). A Critical Analysis of Crack Propagation Laws. Journal of Basic Engineering, 85(4), 528–533. https://doi.org/10.1115/1.3656900

Roe, K. L., & Siegmund, T. (2003). An irreversible cohesive zone model for interface fatigue crack growth simulation. Engineering Fracture Mechanics, 70(2), 209–232. https://doi.org/10.1016/S0013-7944(02)00034-6

Sika Italia SpA. (2019). SikaWrap®-300 C Technical Sheet. September 2019. https://ita.sika.com/content/dam/dms/itgen/l/sikawrap_-300_c.pdf

Yun, Y., Wu, Y.-F., & Tang, W. C. (2008). Performance of FRP bonding systems under fatigue loading. Engineering Structures, 30(11), 3129–3140. https://doi.org/10.1016/j.engstruct.2008.04.026

Zhou, H., Fernando, D., Chen, G., & Kitipornchai, S. (2017). The quasi-static cyclic behaviour of CFRP-to-concrete bonded joints: An experimental study and a damage plasticity model. Engineering Structures, 153, 43–56. https://doi.org/10.1016/j.engstruct.2017.10.007

Zhu, J.-T., Wang, X.-L., Kang, X.-D., & Li, K. (2016). Analysis of interfacial bonding characteristics of CFRP-concrete under fatigue loading. Construction and Building Materials, 126, 823–833. https://doi.org/10.1016/j.conbuildmat.2016.06.071